Anaerobic protein degradation

Effects of protein structural complexity, protein concentrations, carbohydrates, and volatile fatty acids

Deng, Zhe; Ferreira, Ana Lucia Morgado; Spanjers, Henri; van Lier, Jules B.

DOI
10.1016/j.biteb.2023.101501

Publication date
2023

Document Version
Final published version

Published in
Bioresource Technology Reports

Bioresource Technology Reports 22 (2023) 101501

Contents lists available at ScienceDirect

Bioresource Technology Reports

journal homepage: www.sciencedirect.com/journal/bioresource-technology-reports

Anaerobic protein degradation: Effects of protein structural complexity, protein concentrations, carbohydrates, and volatile fatty acids

Zhe Deng [a,b,*], Ana Lucia Morgado Ferreira [b], Henri Spanjers [a], Jules B. van Lier [a]

[a] Delft University of Technology, Department of Water Management, Stevinweg 1, 2628 CN Delft, the Netherlands
[b] Veolia Water Technologies Techno Center Netherlands B.V. - Biothane, Tanthofdreef 21, 2623 EW Delft, the Netherlands

ARTICLE INFO

Keywords:
Anaerobic digestion
Carbohydrates
Modified Gompertz models
Protein
Rate-limiting step
Volatile fatty acids

ABSTRACT

Bovine serum albumin (BSA) and casein (CAS) were used in batch tests to compare the protein degradation in the presence and absence of carbohydrates and volatile fatty acids (VFAs). The modified Gompertz model was applied to estimate reaction rates. The results showed that deamination was the rate-limiting step, with a rate ranging between 2.7 and 12.7 mgN·h^{-1}. Higher protein structural complexity negatively affected protein hydrolysis, deamination, and methanogenesis by a factor of 1.6–3.8; whereas a higher protein concentration improved the conversion rates. A carbohydrate:protein COD ratio of 1 improved the hydrolysis rate of BSA from 26 mg·h^{-1} to 45 mg·h^{-1}, and that of CAS from 98 mg·h^{-1} to 157 mg·h^{-1}; whereas the deamination rate slightly decreased from 2.7 mg N·h^{-1} to 2.5 mg N·h^{-1} and from 6.0 mg N·h^{-1} to 5.6 mg N·h^{-1}. Additionally, an initial VFAs:protein COD ratio of 1 decreased the CAS deamination rate by 17 %.

1. Introduction

The global meat production in 2018 was 342 million tons·year^{-1} (FAO, 2020) and the milk production was 354 million tons·year^{-1} (Eurostats, 2018). More than 30 % of the animal weight ends up as protein-rich waste and 2.5 L of wastewater is produced per L of processed milk, resulting in abundant production of protein-rich waste streams annually (Eurostats, 2018). The protein content can be 40 % of the dry weight in dairy wastewater and 90 % in slaughterhouse wastewater (Salminen and Rintala, 2002; Slavov, 2017). Protein-rich streams have been considered as potential feedstock for biogas production. A lab-scale protein-fed reactor is confirmed to be stable and can produce biogas (Kovács et al., 2013); as such, the protein-rich stream can be used for bioenergy and ammonia recovery (Kovács et al., 2015).

Anaerobic protein degradation can be generalised into three steps, hydrolysis of protein to amino acids, deamination (or acidification) of amino acids into ammonium and volatile fatty acids (VFAs), and methane (CH_4) production from VFAs (i.e., methanogenesis) (McInerney, 1988). The presence of proteins can be problematic in anaerobic digestion (AD), due to 1) occurrence of foaming, 2) incomplete degradation of organic nitrogenous compounds (Bareha et al., 2018), 3) increase in total ammoniacal nitrogen concentration, which may result in inhibition of methanogenesis (Jiang et al., 2019), 4) deterioration of the morphological sludge properties (Liu et al., 2019). According to the reviews of Mata-Alvarez et al. (2014) and Rajagopal et al. (2013), previous studies focus on the inhibition of ammonia/ammonium on methanogens, and attempt to co-digest protein-rich streams with carbohydrate-rich streams to reduce inhibition by preventing a pH rise and increasing the C/N ratio.

In fact, carbohydrates are reported to have a negative impact on protein degradation because they can suppress protease production (Glenn, 1976). Breure et al. (1986) and Yu and Fang (2001) observed that carbohydrate is degraded prior to protein: in their chemostat, glucose was completely acidified whereas gelatine was barely acidified; and in batch reactors, proteins only started to be degraded when carbohydrates were depleted. A possible explanation is that carbohydrates, especially glucose, are thermodynamically preferred by microorganisms since their fermentation yields more energy than fermenting amino acids. Bacterial cells gain 1–2 mol ATP·mol^{-1} glucose compared to 0.5 mol ATP·mol^{-1} amino acids (Barker, 1981; Zhou et al., 2018). Nonetheless, the protein degradation rates in the presence and absence of carbohydrates are not yet investigated, as well as the step that is affected

Abbreviations: AD, anaerobic digestion; BSA, bovine serum albumin; C2, acetate; C3, propionate; C4, butyrate; C5, valerate; CAS, casein; COD, chemical oxygen demand; GEL, gelatine; GLU, glucose; iC4, iso-butyrate; iC5, iso-valerate; iC6, iso-caproate; LAC, lactose; TN, total nitrogen; TS, total solids; VFAs, volatile fatty acids; VS, volatile solids.

* Corresponding author at: Delft University of Technology, Department of Water Management, Stevinweg 1, 2628 CN Delft, the Netherlands.
E-mail address: z.deng-2@tudelft.nl (Z. Deng).

https://doi.org/10.1016/j.biteb.2023.101501
Received 15 May 2023; Received in revised form 8 June 2023; Accepted 8 June 2023
Available online 12 June 2023

by the presence of carbohydrates and limiting the protein conversion.

To optimize the degradation of proteins, it is important to understand the effects of the presence of carbohydrates and their intermediates, i.e., VFAs, on protein degradation, and to identify the rate-limiting step for CH_4 production from protein-rich streams. It is generally agreed that hydrolysis is the rate-limiting step during AD of complex feedstock (Kobayashi et al., 2015), whereas Duong et al. (2019) found that acidification of amino acids is the rate-limiting step during anaerobic digestion of dissolved proteins. Additionally, most methanogens are known to be sensitive to process perturbations and have a slow growth rate (Meegoda et al., 2018). Thus, next to hydrolysis and acidification, methanogenesis is also considered the potential limiting step. However, instead of the CH_4 production rate, previous research mainly focused on the CH_4 potential or yield (Braguglia et al., 2018; Mata-Alvarez et al., 2014).

To identify the rate-limiting step during anaerobic protein degradation, it is essential to compare the rates of the three reaction steps. Previous studies considered either acidification or CH_4 production, the comparison of the three reaction steps was overlooked. Moreover, gelatine (GEL) was the most used model protein, but it is only a mixture of peptides, and it is not representative for the complex structures of most proteins in waste streams. Protein in real wastewaters varies in type and concentration, e.g., casein (CAS) is the most abundant protein in dairy wastewater (80 % of total protein), and it consists of four types of CAS (Atamer et al., 2017); whereas albumin accounts for 55 % of total protein in blood (Smith et al., 2013), and is supposed to be the most abundant in wastewater from animal slaughterhouses. The different types and concentrations of protein also impact the anaerobic digestion performance. For example, although both fish ensilage and manure are regarded protein-rich streams, Vivekanand et al. (2018) reported 4.7 times higher methane yield from fish ensilage than that from manure. According to Elbeshbishy and Nakhla (2012), the methane yield at a protein concentration of 1.0 g COD·L^{-1} is 1.5 times higher than that at a protein concentration of 5.0 g COD·L^{-1}. However, the underlying mechanism is to be revealed.

Our research aimed to investigate the effect of different types of protein, different concentrations of protein, and presence of carbohydrates and VFAs on anaerobic protein degradation. To compare the protein degradation rates of different protein-rich wastewaters, bovine serum albumin (BSA) and CAS, with different structural complexities and representing the main protein in slaughterhouse and dairy wastewater, were used in the experiments. Additionally, the modified Gompertz kinetic model was used to describe and compare the hydrolysis rates, deamination rates, i.e., ammonium release rate during fermentation minus ammonium consumption rate for bacterial growth, and methanogenesis rates, when protein was degraded in the presence and absence of carbohydrates and VFAs.

2. Methods

2.1. Materials and experimental setup

2.1.1. Inoculum and (co-)substrates

The inoculum used in this study was collected from an anaerobic digester of a full-scale treatment plant in the Netherlands. The inoculum had an average total solids (TS) and volatile solids (VS) content of 155 ± 10 g·kg^{-1} wet weight and 120 ± 1 g·kg^{-1} wet weight, respectively. The inoculum was stored at room temperature and was washed three times with tap water before use.

Two model proteins were used: bovine serum albumin (BSA, A7030, Sigma Aldrich, Germany) and CAS (9000-71-9, Fisher Scientific, Germany). Likewise, two model carbohydrates were used: D-(+)-Glucose (GLU, G8270, Sigma Aldrich, Germany) and α-Lactose monohydrate (LAC, L3625, Sigma Aldrich, Germany). Acetate (C2, Sigma Aldrich, Germany) and propionate (C3, Sigma Aldrich, Germany) served as model VFAs. Gelatine (GEL, G2500, Sigma Aldrich, Germany) was used as a positive control for proteins, because it is widely used as a representative protein in wastewaters and has a high biodegradability (Breure and Van Andel, 1984; Duong et al., 2019). BSA and GLU were used to represent the main protein and carbohydrate in slaughterhouse wastewater, especially from the slaughter line (Ruiz et al., 1997). CAS and LAC were used to represent the main protein and carbohydrate in dairy wastewater. The VFA compositions (C2: C3 was 1:3, based on chemical oxygen demand (COD)) were determined based on the composition found in pre-acidified dairy wastewater in Biothane – Veolia Water Technologies Techno Center Netherlands B.V Research Facilities (Delft, The Netherlands).

The characteristics of the four protein feeds and six co-substrate feeds are listed in Table 1, the target COD of the feeds was 6.0 g·L^{-1}, or, in the case of the low concentration protein feeds BSA_1 and CAS_1, 3 g·L^{-1} (Table 1). The concentration of protein and carbohydrate used in our study were based on the measurement of real slaughterhouse and dairy wastewaters. The reference wastewaters, with a total COD of 5000–6500 mg·L^{-1} and a protein content of 50 % COD, were described in details in the study of Deng et al. (2023) and Tan et al. (2021). The protein concentration in the BSA_2 and CAS_2 was twice that in the BSA_1 (and BSA_1 co-substrates feeds) and CAS_1 (and CAS_1 co-substrates feeds). The total nitrogen (TN) of the added protein is also listed in Table 1. NH_4Cl was added to adjust the COD: N ratio of the co-substrate feeds to 10–11, which was the same as pure protein feeds. Due to the heterogeneity of the casein solution and potential systematic COD measurement error, there was a variation of 3–15 % difference among the total COD of the CAS and co-substrate feeds.

Table 1
Composition and characteristics of the blank, control (GEL), five BSA feeds and five CAS feeds.

Feeds	COD (%)			COD	[c]TN (mg·L^{-1})
	Protein	Carbohydrate	VFAs	(g·L^{-1})	(mg·L^{-1})
[a]Blank	0	0	0	0	0
[b]GEL	100	0	0	6.0 ± 0 %	936 ± 4 %
1 BSA_2	100	0	0	6.2 ± 0 %	804 ± 9 %
2 BSA_1	100	0	0	3.2 ± 1 %	322 ± 2 %
3 BSA_1 + GLU	50	50	0	6.0 ± 0 %	395 ± 0 %
4 BSA_1 + GLU + VFA	50	25	25	6.2 ± 1 %	312 ± 1 %
5 BSA_1 + VFA	50	0	50	6.2 ± 0 %	318 ± 3 %
6 CAS_2	100	0	0	7.8 ± 0 %	809 ± 9 %
7 CAS_1	100	0	0	3.2 ± 1 %	292 ± 3 %
8 CAS_1 + LAC	50	50	0	6.8 ± 0 %	465 ± 0 %
9 CAS_1 + LAC + VFA	50	25	25	5.6 ± 1 %	334 ± 6 %
10 CAS_1 + VFA	50	0	50	5.2 ± 0 %	355 ± 5 %

Feed 1, 2, 6, and 7 were the pure protein substrate, feed 1 and 6 had a protein concentration twice as that of feed 2 and 7, as indicated by the subscription.
Feed 3–5, with the same BSA protein concentration as in feed 2, were BSA_1 co-substrates.
Feed 8–10, with the same CAS protein concentration as in feed 7, were CAS_1 co-substrates.
[a] Only inoculum and $NaHCO_3$ buffer were added to the blank.
[b] GEL was used as a positive control, blank and control were used to validate the CH_4 production registration. Blanks should be below 20 % of total methane production in the positive control, and methane production in positive control shall be between 85 % and 100 % of the theoretical biomethane potential (BMP) (Holliger et al., 2016).
[c] TN is the total nitrogen of added protein.

The macronutrients added were 20 mg·L^{-1} of KH_2PO_4 (7778-77-0, Sigma Aldrich, the Netherlands) 15 mg ·L^{-1} of $MgSO_4{\cdot}7H_2O$ (10034–99-8, Sigma Aldrich, the Netherlands), and 10 mg ·L^{-1} of $CaCl_2$ (10043–52-4, Sigma Aldrich, the Netherlands). The pH of the feeds was adjusted to 7.5 with 0.1 mol·L^{-1} NaOH or HCl solutions, and finally 3.5 g·L^{-1} of $NaHCO_3$ (144–55-8, Sigma Aldrich, the Netherlands) was added as a buffer.

2.1.2. Anaerobic batch test

Batch tests were carried out in duplicates with 600 mL glass bottles, the working volume was 500 mL, and the headspace was 100 mL. In each bottle, 44 g of inoculum and one feed were added, resulting in an initial biomass concentration of 12 gVS·L^{-1} and a feed COD concentration of 6 g·L^{-1} (3 g·L^{-1} for BSA_1 and CAS_1). Hereafter the bottles were closed with a screw cap and butyl rubber septum and flushed with nitrogen gas for 1 min before incubation at 37 °C and under continuous stirring at 100 rpm.

2.2. Sampling and analysis

Liquid sampling was carried out at 1 h, 15 h, 25 h, 45 h, 70 h, and 140 h with a syringe. Samples were analysed for pH, COD, TN, NH_4^+-N, VFA composition, and protein. After pH measurement, samples were first centrifuged at 13,500 ×*g* for 5 min and filtered through 0.45 μm membrane filters (Whatman, Sigma Aldrich, the Netherlands). COD, TN, and NH_4^+-N were measured with HACH-Lange kits (Sigma Aldrich, the Netherlands) LCK014, LCK338, and LCK302, respectively.

Protein concentrations were assessed following the manufacturer protocol of the bicinchoninic acid kit (BCA protein assay, BCA1-1KT, Sigma Aldrich), measured by a spectrometer at 562 nm, with either BSA or CAS as standard.

The VFAs composition, including C2, C3, C4 (butyrate), iC4 (iso-butyrate), C5 (valerate), iC5 (iso-valerate), iC6 (iso-caproate), was analysed by a gas chromatograph (GC, 7820A, Agilent Technologies, Netherlands) equipped with a CP 7614 column (WCOT Fused Silica 25 m × 0.55 mm, CP-wax 58 FFAP capillary, Agilent Technologies) and flame ionization detector. The injector temperature was 250 °C, and nitrogen gas (28.5 mL·min^{-1}) with a split ratio of 10 was used as a carrier. The GC oven method sequence was started at 100 °C, held for 2 min; and then increased to 140 °C and held for 6 min. An internal standard was prepared with 100 mg·L^{-1} iC5 in 5 % formic acid. Cumulative CH_4 production (mL) was recorded every hour with AMPTS-II (BPC Instruments, Sweden), and converted to mg COD using 0.35 L CH_4 = 1 g COD .

The hydrolysis, deamination, and methanogenesis rates were described by the modified Gompertz model, which has been widely used for describing the biogas production process (Liu et al., 2023). The used equations and parameters are presented in Table 2. The nonlinear least-squares method was used for model fitting in MATLAB (R2016b), and the coefficient of determination (R^2) and root-mean-square error (RMSE) were used to evaluate the goodness of the fit (details of results can be found in Fig. S_1).

Table 2
Modified Gompertz models used to describe the hydrolysis, deamination and methanogenesis rates.

Step	Equation	Parameters
Hydrolysis	$P_{(t)} = P_m \times exp\left(-exp\left[\frac{R_P \times e}{P_m}(\lambda - t) + 1\right]\right)$	P_m, R_P, λ
Deamination	$N_{(t)} = N_m \times exp\left(-exp\left[\frac{R_N \times e}{N_m}(\lambda - t) + 1\right]\right)$	N_m, R_N, λ
Methanogenesis	$C_{(t)} = C_m \times exp\left(-exp\left[\frac{R_C \times e}{C_m}(\lambda - t) + 1\right]\right)$	C_m, R_C, λ

P_m, N_m and C_m represent the maximum hydrolysed protein (mg), ammonium production (mg N) and methane production (mg COD), respectively.
R_P, R_N and R_C represent the maximum reaction rates (mg·h^{-1}) of hydrolysis, deamination and methanogenesis following the Modified Gompertz model, respectively.
λ is the delay of the reaction (h).

3. Results and discussion

3.1. Effect of protein structural complexity and protein concentration

To compare protein degradation in the different protein-rich wastewaters, the tertiary-structured BSA and simple secondary-structured CAS, were used in the batch tests. In addition, the effect of protein concentrations on the conversion rates was studied. The added protein concentrations in the BSA_2 and CAS_2 were twice that in the BSA_1 and CAS_1, while the COD in the BSA_2 and CAS_2 was 6.0 g·L^{-1}, and the COD in the BSA_1 and CAS_1 was 3.0 g·L^{-1}.

3.1.1. Hydrolysis

Fig. 1A shows the degraded protein (mg) in BSA_1 and BSA_2 at each sampling time. The degraded protein was calculated as initial protein minus the measured protein; results of the duplicates are presented together with simulated results. Fig. 1A also presents the reaction rate obtained from the modified Gompertz model fitting. Results clearly show that the protein hydrolysis rate in BSA_2 (75 ± 28 mg·h^{-1}, the obtained reaction rates were present with a 95 % confidence bound) was higher than in BSA_1 (26 ± 9 mg·h^{-1}). Fig. 1B shows the degraded protein (mg) in CAS_1 and CAS_2, as well as the obtained reaction rates. Like in the BSA incubations, CAS_2 also had a somewhat higher hydrolysis rate than CAS_1, which were 155 ± 173 mg·h^{-1} and 98 ± 79 mg·h^{-1}, respectively, but observed differences were much less than with BSA.

The higher initial protein concentrations in BSA_2 and, to a lesser extent, CAS_2 led to a higher hydrolysis rate. According to Guo et al. (2021), protease activity is induced by protein concentration and consequently higher protein concentration leads to higher protease activity, and therefore higher hydrolysis rate. Additionally, the hydrolysis rates of BSA substrates were 2.0–3.8 times lower than that of CAS substrates, indicating a negative impact of protein structural complexity on the protein hydrolysis rate. Notably, the difference of protein concentration between the duplicates was 200–500 mg·L^{-1} and 400–600 mg·L^{-1} in BSA_2 and CAS_2, as a result, the hydrolysis rate given by the modified Gompertz model had a wide 95 % confidence bound. To have an accurate protein hydrolysis rate, a better protein measurement is needed, especially at high protein concentrations (e.g., 6000 mg·L^{-1}) and when proteins have a lower solubility (e.g., casein).

3.1.2. Deamination

Fig. 1C presents the produced ammonium (mg N) in BSA_1 and BSA_2 at each sampling time. The ammonium consumption was ignored, because it is low in anaerobic digestion of protein rich wastes, i.e., about 5 % of the COD is used for bacterial growth, and the C:N ratio of the biomass is 5:1 (van Lier et al., 2020). As shown in the figure, the reaction rates obtained from the modified Gompertz model clearly showed that BSA_2 had a deamination rate 2.1 times higher than that of BSA_1, which were 5.7 ± 2 mg N·h^{-1} and 2.7 ± 0.6 mg N·h^{-1}, respectively. In addition, a lower percentage (84 %, calculated as produced ammonium in mg N divided by TN in mg N in the initial protein) of the initial protein in BSA_2 was converted to ammonium at the end of the experiment (140 h), compared to that of BSA_1 (91 %).

Fig. 1D shows the produced ammonium (mg N) in CAS_1 and CAS_2 at each sampling time. The reaction rates obtained from the modified Gompertz model were 12.7 ± 5 mgN·h^{-1} in CAS_2 and 6.0 ± 1 mgN·h^{-1} in CAS_1, respectively. In CAS_2, 97 % of the nitrogen in the added protein was released as ammonium, and 100 % of nitrogen in the added protein in CAS_1 was released as ammonium.

Like hydrolysis, CAS showed about 2.2 times higher deamination rate than BSA at the same initial protein concentrations. The protein hydrolysis and deamination of CAS stabilized at approximately 50–70 h,

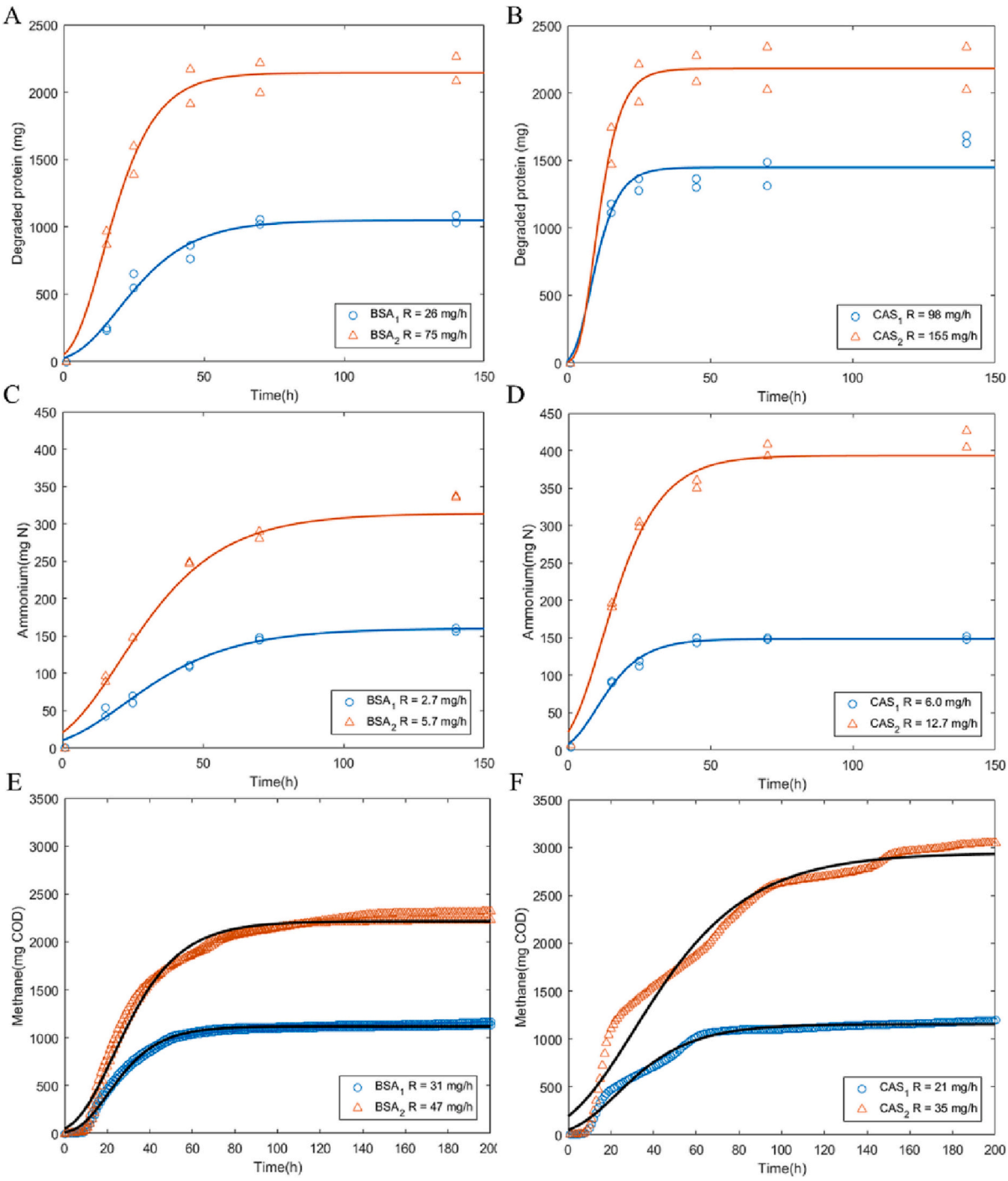

Fig. 1. Profile and reaction rates of A) BSA hydrolysis and B) CAS hydrolysis, C) BSA deamination and D) CAS deamination, E) BSA methanogenesis and F) CAS methanogenesis in pure protein feeds. Measurements of duplicates were presented as scattered plot, and modelled values were presented as solid lines, along with the overall reaction rates ($mg{\cdot}d^{-1}$) of hydrolysis, deamination and methanogenesis obtained from the modified Gompertz models. BSA_1 and CAS_1 indicated a substrate protein COD concentration of 3 $g{\cdot}L^{-1}$, and BSA_2 and CAS_2 indicated a substrate protein COD concentration of 6 $g{\cdot}L^{-1}$.

whereas it took 70–100 h for the deamination of BSA. According to Bhat et al. (2016) and Bevilacqua et al. (2020), the conversion of proteins can be affected by the protein structure or the amino acids compositions. However, the effect of protein structural complexity and amino acids composition on the protein conversion rate was not investigated before. The β-CAS used in this study had a plain secondary structure (Dickinson, 2003), making it structurally simpler compared to the tertiary-structured BSA (Varga et al., 2016). Consequently, the protease was able to more efficiently break down the peptide linkages in CAS, requiring less energy and time compared to the unfolding of the BSA peptide chain to release the amino acids and amino groups. With a sequence length of 607 amino acids for BSA and 225 amino acids for CAS, the interactions among BSA amino acid side chains are more intricate, contributing to the reported inert nature of BSA (Bourassa et al., 2010). The lower degradation rate of BSA was attributed to the higher structural complexity. Based on the amino acids composition (in % of mass) in BSA and CAS (GMIA, 2019; Nightingale et al., 2017), the major difference is the fraction of cysteine. Cysteine accounts for 5.51 % of amino acids in BSA, whereas it is 0.00 % in CAS. Cysteine is known to form intramolecular and intermolecular di-sulphide bonds and is the key

contributor to protein strength and rigidity (Miniaci et al., 2016), e.g., the structural protein, keratin, contains 7–20 % cysteine (Numata, 2021). In conclusion, the higher fraction of cysteine in BSA, which very likely contributed to a higher protein structural complexity, may have resulted in the observed lower degradation rate.

3.1.3. Methanogenesis

The methane production in the positive control (GEL) was 96 % of the added COD, and the CH_4 production in the blank was 12 % of that in the positive control.

Fig. 1E shows the cumulative CH_4 production (mg COD) in BSA_1 and BSA_2. Based on the modified Gompertz model, BSA_2 had a higher overall methanogenesis rate (during 0–200 h incubation time) of 47 ± 1 mg $COD{\cdot}h^{-1}$ than that of BSA_1, which was 31 ± 1 mg $COD{\cdot}h^{-1}$. However, it should be noted that the modified Gompertz model was not able to fully capture all the experimental data. BSA conversion did not follow the expected first-order reaction kinetics, especially at the high BSA concentration. To evaluate the conversion of protein to CH_4, the conversion efficiency was calculated by dividing the cumulative CH_4 production (mg COD) at 140 h by the initial COD (mg). BSA_2 and BSA_1 had a similar conversion efficiency of 70–71 %. The conversion efficiency of protein to CH_4 was not affected by the initial protein concentration in the absence of carbohydrates.

Fig. 1F shows the cumulative CH_4 production (mg COD) in CAS_1 and CAS_2. As obtained from the modified Gompertz model, the overall methanogenesis rate in CAS_2 was 35 ± 2 mg $COD{\cdot}h^{-1}$ and that of CAS_1 was 21 ± 1 mg $COD{\cdot}h^{-1}$. However, compared to BSA, the deviation from the first-order reaction kinetics was much larger in the case of CAS as the substrate. In addition, the COD to CH_4 conversion efficiency of CAS_2 (75 %) was slightly higher than that of CAS_1 (72 %). Based on the overall methanogenesis rate of CAS, the initial protein concentration had a slightly positive effect on the CAS conversion to CH_4 rate and efficiency.

Regardless of the type and concentration of proteins, the four protein feeds all showed a lag phase of approximately 10 h, as shown in Fig. 1E and F. The CH_4 production profiles of CAS_2 and CAS_1 showed two different stages with distinct rates: an initial rapid production stage followed by a much slower production stage. CAS_1 and CAS_2 showed a substantially lower CH_4 production rate during 20–100 h, simultaneously, VFAs accumulation was observed. As shown in Fig. 2A and B, the total VFA concentrations in BSA_1 remained at a level of 100 mg $COD{\cdot}L^{-1}$ during 0–70 h, whereas the total VFA in CAS_1 quickly increased to 440 mg $COD{\cdot}L^{-1}$ at 15 h, and remained between 350 and 500 mg $COD{\cdot}L^{-1}$ until 45 h. Although the measured VFA concentration was likely not inhibiting at a pH above 7 (Siegert and Banks, 2005), the VFA accumulation and concomitantly lower methanogenesis rate suggested a negative effect of CAS, being a protein with a simpler structure, on the methanogenesis rate (Figs. 1F, 2B).

This seemingly staged conversion could indicate the presence of two different CAS protein fractions: one fraction was easily degradable and showed a fast CH_4 production ($0-20h$), whereas the other fraction showed slower CH_4 production ($20-100h$). After 100 h of incubation, a third even slower conversion could be identified, possibly indicating a third protein fraction. Results suggest that methanogenesis could have been the rate-limiting step during 0–20 h, but step(s) prior to methanogenesis were certainly limiting the methane production during 20–100 h.

In this study, the cumulative methane production profile was divided into two different stages, which were modelled separately for obtaining a better estimation of the maximum methane production rate (Fig S_1). The incubation period of 0–40 h in BSA batch tests and 0–20 h in CAS batch tests were designated as the rapid reaction stage, during which the high reaction rate was modelled; concurrently, the 40–200 h for BSA and 20–200 h for CAS were designated as the slow reaction stage, characterized by a low reaction rate. By modelling the two methane production stages separately, the lag phase given by the model was close to 10 h and the R^2 was significantly improved (Table S_1). The results of the high and low methane production rates are shown in Table 3. Notably, the overall methanogenesis rate of BSA was about 25 % - 30 % higher than that of CAS at the same initial protein concentrations, but the maximum methanogenesis rate of BSA was 40 % - 46 % lower than that of CAS at the same initial protein concentration. Therefore, it was concluded that a high protein structural complexity had a negative effect on the maximum methanogenesis rate, and a higher protein concentration had a positive effect on the methanogenesis.

In summary, compared to the reaction rates of hydrolysis and methanogenesis, the deamination rates were found to be the lowest with both BSA and CAS as the substrates. Additionally, as shown in Fig. 2 (blue bars), the increase of VFAs was below 100 mg·L^{-1} after 15 h, indicating minor accumulation of VFAs during this period. Therefore, deamination was potentially the rate-limiting step during the degradation of BSA and CAS, especially after 20 h of batch incubation. The applied protein measurement considered all non-monomers, i.e., protein and peptides, and gave a good indication of the hydrolysis of protein to amino acids. Measuring the protein concentration in time series can be a proper method to describe the protein hydrolysis rate. However, it is recommended to include amino acids measurement in future studies to

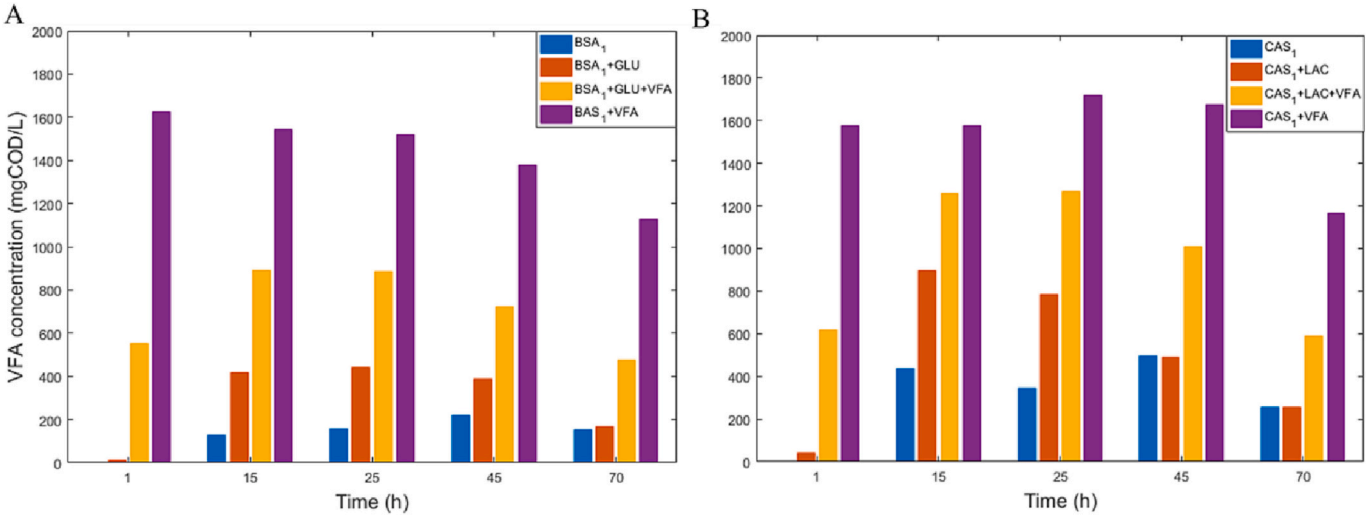

Fig. 2. Total VFA concentrations (in mg $COD{\cdot}L^{-1}$) in A) BSA incubations, and B) CAS incubation, at different time instants during the batch tests. Incubations consisted of pure proteins, as well as proteins with co-substrates (GLU = glucose, LAC = lactose, VFA = volatile fatty acids).

Table 3
Methanogenesis rate (in mg·h^{-1}) during the fast and slow methane production stages with 95 % confidence bounds.

	BSA_2	BSA_1	BSA_1 + GLU	BSA_1 + GLU + VFA	BSA_1 + VFA
Overall reaction rate (mg·h^{-1})	47 ± 1	31 ± 1	78 ± 2	49 ± 2	22 ± 1
High reaction rate (mg·h^{-1})	66 ± 3	34 ± 1	99 ± 8	85 ± 6	48 ± 2
Low reaction rate (mg·h^{-1})	26 ± 2	24 ± 4	36 ± 3	41 ± 2	21 ± 1
	CAS_2	CAS_1	CAS_1 + LAC	CAS_1 + LAC + VFA	CAS_1 + VFA
Overall reaction rate (mg·h^{-1})	35 ± 2	21 ± 1	72 ± 4	37 ± 2	20 ± 1
High reaction rate (mg·h^{-1})	122 ± 3	57 ± 2	181 ± 12	95 ± 4	45 ± 4
Low reaction rate (mg·h^{-1})	23 ± 1	19 ± 1	33 ± 1	23 ± 1	18 ± 1

The overall reaction rate is the average methanogenesis rate during 0–200 h. The high reaction rate is the methanogenesis rate during 0–40 h in BSA batch tests and 0–20 h in CAS batch tests; concurrently, the low reaction rate is the methanogenesis rate during 40–200 h and or 20–200 h, for BSA and CAS, respectively.

examine the accumulation of amino acids.

Besides, our results clearly showed that the applied modified Gompertz model, which is based on first-order conversion kinetics, was not able to describe the two-three different stages of CAS degradation, the computed results were an average of the entire conversion. It is suggested to model the different degradation stages separately or develop a model that can describe protein conversion with different degradation stages, to better estimate the maximum methane production rates.

3.2. Effect of glucose, lactose and volatile fatty acids

To investigate the effect of the presence of carbohydrates and their intermediates (i.e., VFAs) on anaerobic protein degradation, GLU or LAC and VFAs were added to be co-digested with the model proteins, BSA and CAS. The protein hydrolysis, deamination and methanogenesis rates were compared between pure protein feeds and co-substrates feeds.

3.2.1. Hydrolysis

Fig. 3A shows the degraded BSA protein (mg) in all BSA_1 and co-substrate incubations; measurements of the duplicates are shown in scattered plots, with the modelled results as solid lines. Based on the obtained reaction rates from the modified Gompertz model, BSA_1 + GLU had the highest hydrolysis rate (45 ± 35 mg·h^{-1}), followed by BSA_1 + GLU + VFA (32 ± 15 mg·h^{-1}), whereas BSA_1 + VFA had a similar hydrolysis rate (24 ± 7 mg·h^{-1}) as BSA_1 (26 ± 9 mg·h^{-1}).

Fig. 3B shows the degraded CAS protein (mg) in all CAS_1 and co-substrate incubations; duplicate measurements are shown as scattered plots, with solid lines representing the modelled results. The reaction rates obtained from the modified Gompertz model are also shown in the figure. Like the batch test with BSA, CAS_1 + LAC had the highest hydrolysis rate (157 ± 185 mg·h^{-1}), and the CAS_1 + VFA had a similar hydrolysis rate (99 ± 80 mg·h^{-1}) as CAS_1. However, CAS_1 + LAC+VFA had the lowest hydrolysis rate of 94 ± 165 mg·h^{-1}.

Contrary to previous studies reporting an inhibition behaviour of carbohydrates on protein hydrolysis (Yang et al., 2015; Yu and Fang, 2001), the presence of GLU and LAC improved the BSA and CAS hydrolysis rates by a factor of 1.6–1.7 in this study, indicating a positive effect on protein hydrolysis. The present results are in agreement with the study of Elbeshbishy and Nakhla (2012), in which 1.5 fold higher hydrolysis rate was observed when starch was added in anaerobic degradation of BSA. In addition, the carbohydrate:protein ratio is 1 in terms of COD in our study. Wang et al. (2022) reported that such a carbohydrate to protein ratio optimizes protease activity. In contrast, the carbohydrate to protein ratios in previous studies were either below or above 1, resulting in reduced protease activity and consequently lower hydrolysis rates (Yang et al., 2015, Yu and Fang, 2001). The presence of VFAs had an ignorable effect on protein hydrolysis, whereas the co-presence of carbohydrates and VFAs had a negative effect on CAS hydrolysis. Duong et al. (2022) reported an inhibition effect of VFAs on gelatine hydrolysis at a VFA:GEL COD ratio of 2.2. Likely, the synergetic effect of a lower protease activity and VFA inhibition at a CAS:LAC:VFA COD ratio of 1:0.5:0.5 lead to the lower hydrolysis rate in CAS_1 + LAC+VFA. Whereas in BSA_1 + GLU + VFA, the BSA hydrolysis rate and acidification rate were lower than that of CAS (Fig. 2), and therefore the protein hydrolysis was not inhibited by VFAs at a lower concentration.

3.2.2. Deamination

Fig. 3C presents the ammonium production (mg N) in all BSA_1 and co-substrate incubations at each sampling time. The obtained reaction rates applying modified Gompertz model fittings are shown in the same figure. The deamination rates of BSA_1 + GLU, BSA_1 + GLU + VFA and BSA_1 + VFA were 2.5 ± 0.2 mg N·h^{-1}, 2.9 ± 0.5 mg N·h^{-1}and 2.6 ± 0.9 mg N·h^{-1}, respectively. The lowest value found for BSA_1 + GLU (7 % lower than solely BSA_1) indicated that the presence of glucose had a slightly negative effect on the BSA deamination. Both the deamination rates of BSA_1 + GLU and BSA1 + VFA were lower than solely BSA_1, whereas the deamination rates of BSA_1 + GLU + VFA was 7 % higher. The observed phenomenon may be attributed to the initial concentrations of GLU and VFA. Specifically, in the BSA_1 + GLU + VFA batch test, the COD contents of GLU and VFA were half that of BSA_1 + GLU and BSA_1 + VFA batch tests. According to Duong et al. (2022), the activity of methanogens helps mitigate the negative impact of starch on protein deamination. The moderate concentrations of GLU and VFA in BSA_1 + GLU + VFA could have activated the acid-forming bacteria and methanogens, and resulting in a positive effect on the deamination reaction.

In Fig. 3D, the ammonium production (mg N) in all CAS_1 and co-substrate incubations at each sampling time is shown, as well as the reaction rates of the modified Gompertz model. The deamination rates of CAS_1 + LAC, CAS_1 + LAC+VFA, and CAS_1 + VFA were 5.6 ± 2 mg N·h^{-1}, 5.3 ± 2 mg N·h^{-1}, and 5.0 ± 3 mg N·h^{-1}, respectively. The presence of LAC alone led to a 7 % lower deamination rate compared to CAS_1, the presence of both LAC and VFAs caused a 12 % lower deamination rate compared to that of CAS_1, and the presence of VFAs alone led to a 17 % lower deamination rate. The presence of LAC had a minor impact on the CAS deamination, whereas VFAs had a negative effect on the CAS deamination rates.

Both the presence of glucose and lactose showed a negative effect on BSA and CAS deamination. As also observed by Duong et al. (2022), deamination rate reduced to 40 % at a starch:GEL COD ratio of 1. In all our incubations, the pH was maintained above 7 (Fig. S_2), and the C2-iC6 VFA composition did not vary notably during the experiment (data not shown), only a delay in VFA production was observed in BSA_1 + VFA and CAS_1 + VFA (Fig. 2A and B), which indicated that VFA production (i.e., deamination) was negatively affected by the presence of high initial VFA concentration. Possibly, the excessively available VFAs inhibited the protein hydrolysis and affected the bioactivity of the acid-forming bacteria, and therefore limited the acidification of CAS (Duong et al., 2022; Wang et al., 2022).

3.2.3. Methanogenesis

Fig. 3E presents the cumulative CH_4 production (mg COD) in BSA_1 co-substrate and BSA_1 incubations, as well as the obtained methanogenesis rates from the modified Gompertz model. Again, the model was not able to capture the data accurately. The highest deviation was found in incubations with the BSA_1 + GLU + VFA, which had two-three methane production stages with different rates. Therefore, the overall

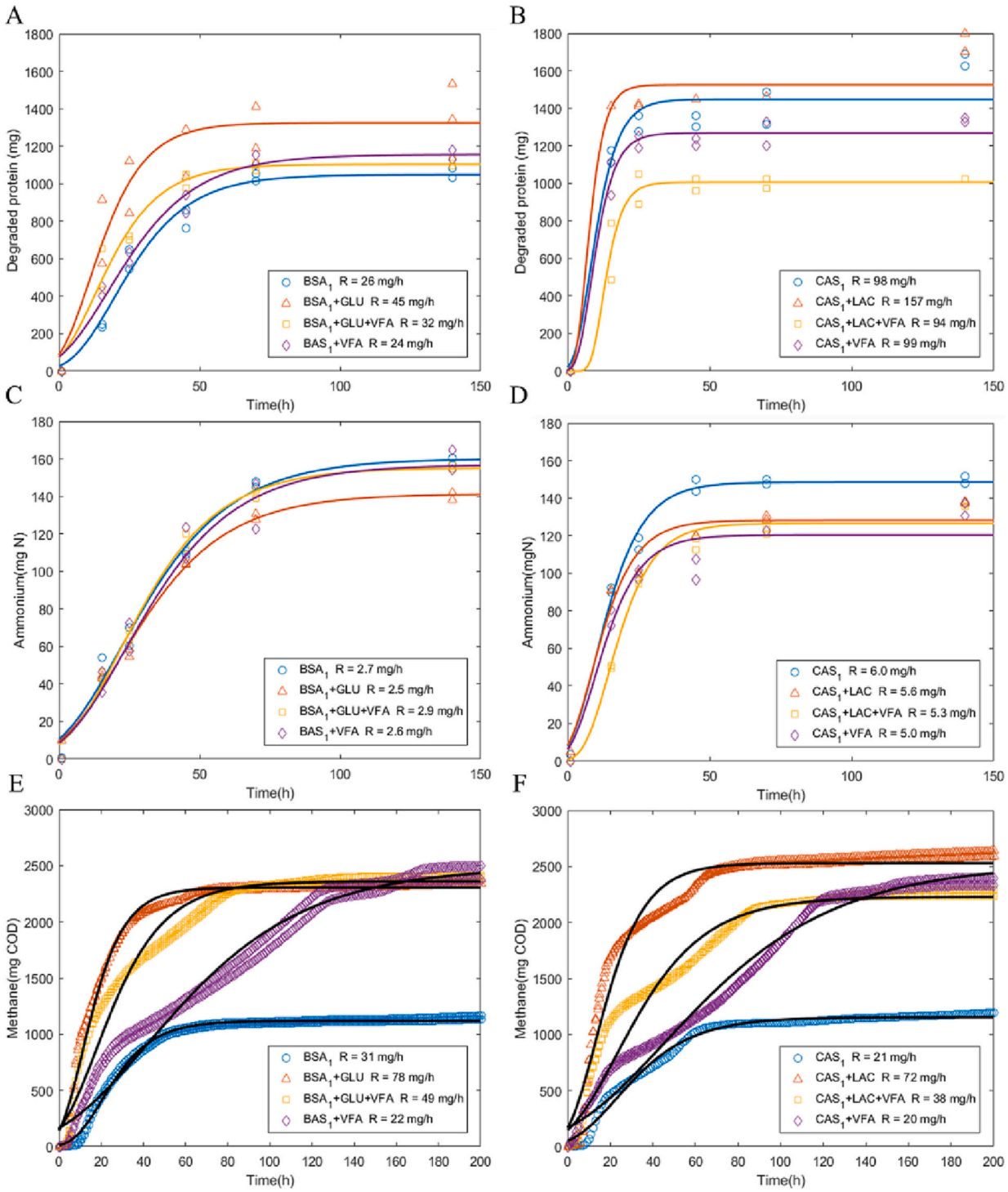

Fig. 3. Profile and reaction rates of protein hydrolysis. Fig. 3A and B, deamination, Fig. 3C and D, and methanogenesis, Fig. 3E and F, in BSA_1 and CAS_1 co-substrates incubations, respectively, compared with BSA_1 and CAS_1 as the sole substrate. Measurements of duplicates were presented as scattered plot, and modelled values were presented as solid lines, along with the overall reaction rates ($mg{\cdot}d^{-1}$) of hydrolysis, deamination and methanogenesis obtained from the modified Gompertz models. (GLU = glucose, LAC = lactose, VFA = volatile fatty acids).

methanogenesis rate estimated by the model was rejected, and instead, the maximum methanogenesis rate was used for comparison (data shown in Table 3). The presence of GLU had a significant positive effect on methanogenesis, the maximum methanogenesis rate in BSA_1 + GLU and BSA_1 + GLU + VFA was 99 ± 8 mg $COD{\cdot}h^{-1}$ and 85 ± 6 mg $COD{\cdot}h^{-1}$, which was 2.5–2.9 times higher than that in the BSA_1 incubation (34 ± 1 mg $COD{\cdot}h^{-1}$). The maximum methanogenesis rate in BSA_1 + VFA was 48 ± 2 mg $COD{\cdot}h^{-1}$, indicating that the presence of high initial VFAs concentration also had a slightly positive effect on the methanogenesis. Additionally, the lag phase in the BSA_1 co-substrates incubations were shorter than that in the BSA_1 incubation, indicating that methanogenesis of protein started later than that of the GLU and VFAs.

Fig. 3F shows the cumulative CH_4 production (mg COD) in CAS_1 with co-substrate incubations and CAS_1 as the sole substrate, along with the overall methanogenesis rates obtained from the modified Gompertz

model. Like the results of the BSA batch tests, the modified Gompertz model also showed a high deviation from the measured data, and the overall methanogenesis rate was regarded as not representative of the methanogenesis step. Therefore, the fast methane production stage was fitted separately to obtain the maximum methanogenesis rate (see Table 3). CAS_1 + LAC showed the highest methanogenesis rate of 181 ± 12 mg COD·h^{-1}, followed by CAS_1 + LAC+VFA, with a rate of 95 ± 4 mg COD·h^{-1}. Although the maximum methanogenesis rate in CAS_1 + VFA (45 ± 4 mg COD·h^{-1}) was lower than that in CAS_1 (57 ± 2 mg COD·h^{-1}), it showed the shortest lag phase of less than 5 h (Fig. 3F). The pH was maintained between 7.0 and 8.0 in all incubations (Supplementary Fig. S_2), being in the optimal range for methanogenesis (Jones et al., 1987). The reduced methanogenesis rate in CAS_1 + VFA might have been caused by the high initial propionate concentration of 1500 mg·L^{-1} (Fig. 2B). Notably, propionate concentrations exceeding 900 mg·L^{-1} at pH 7.0 may lead to inhibition of methanogens, resulting in VFAs accumulation (Wang et al., 2009). In general, the presence of LAC increased the methanogenesis rate by 3.2 times, and the high initial VFA concentrations had a negative effect on the methanogenesis rate but a positive effect on shortening the lag phase.

Like the tests with sole proteins (Section 3.1.3, Fig. 1F), fast and slow methane production stages were observed in the CH_4 production profiles of CAS_1 co-substrates. Moreover, a staged pattern was more clearly observed with BSA_1 co-substrates compared to BSA_1 as the sole substrate, particularly when VFA was added as a co-substrate (Fig. 3E). Likely, methane was mainly produced from the available carbohydrates and VFA in the fast production stage, whereas methane was produced from proteins during the slow production stage and at the end of the slow production stage (Fig. S_3). As already mentioned in Section 3.1.3, methanogenesis was seemingly the rate-limiting step during the fast methane production stage. However, steps prior to methanogenesis were limiting the degradation rate during the slow production stage. Hence, further study is needed to investigate the reaction rates of the intermediates degradation prior to methanogenesis.

Based on our present results, it can be concluded that degradation of intermediates, i.e., deamination, was the rate-limiting step in the presence and absence of carbohydrates and VFAs. It must be noted that commonly, hydrolysis is considered to be the rate-limiting step in AD (Pavlostathis and Giraldo-Gomez, 1991), and therefore solid-state digesters are designed based on attainable hydrolysis rates. However, in the anaerobic treatment of wastewaters from dairy processing or slaughterhouses, deamination is apparently limiting the conversion of proteins to CH_4. Therefore, it can be postulated that reactor designs, e.g., dilution rate or hydraulic retention times, should be based on attainable deamination rate. Moreover, VFAs showed a negative effect on protein hydrolysis and deamination, therefore, high VFA concentrations should be avoided to achieve high reaction rates during protein degradation.

4. Conclusions

Deamination of protein was identified as the rate-limiting step. Compared to CAS, BSA showed lower hydrolysis and deamination rates, suggesting that proteins with a higher structural complexity have a lower degradation rate. Reaction rates obtained from the modified Gompertz model also showed that carbohydrates had a positive effect on the protein hydrolysis rate and methanogenesis rate, but a negative effect on the deamination rate. A high initial VFA concentration had a negative effect on the protein hydrolysis and deamination rates. It is postulated that the design of anaerobic reactors, treating protein-rich wastewaters, should be based on the attainable deamination rate, and high VFA concentrations must be avoided.

CRediT authorship contribution statement

Zhe Deng: Conceptualisation, Investigation, Formal analysis, Writing – Original Draft. **Ana Lucia Morgado Ferreira**: Validation, Supervision, Writing – Review & Editing. **Henri Spanjers**: Conceptualisation, Supervision, Writing – Review & Editing. **Jules B. van Lier**: Conceptualisation, Supervision, Writing – Review & Editing. All authors read and approved the final manuscript.

Declaration of competing interest

The authors declare that they have no known competing financial interests or personal relationships that could have appeared to influence the work reported in this paper.

Data availability

All data generated or analysed during this study are included in this published article and its supplementary information files.

Acknowledgment

This work was supported by the China Scholarship Council under the State Scholarship Fund (No. 201708450043) and Biothane - Veolia Water Technologies Techno Center Netherlands B.V Research Facilities. The authors would like to acknowledge the technical and analytical support given by Patrick van der Linde and Rewin Pale (Biothane, The Netherlands), and thank MSc student Fabian Bodenlenz (Delft University of Technology, The Netherlands) for his contribution to the experiments.

Appendix A. Supplementary data

Supplementary data to this article can be found online at https://doi.org/10.1016/j.biteb.2023.101501.

References

Atamer, Z., Post, A.E., Schubert, T., Holder, A., Boom, R.M., Hinrichs, J., 2017. Bovine β-casein: Isolation, properties and functionality. A review. Int. Dairy J. 66, 115–125.
Bareha, Y., Girault, R., Jimenez, J., Trémier, A., 2018. Characterization and prediction of organic nitrogen biodegradability during anaerobic digestion: a bioaccessibility approach. Bioresour. Technol. 263 (February), 425–436.
Barker, H.A., 1981. Amino acid degradation by anaerobic bacteria. Annu. Rev. Biochem. 50, 23–40.
Bevilacqua, R., Regueira, A., Mauricio-Iglesias, M., Lema, J.M., Carballa, M., 2020. Protein composition determines the preferential consumption of amino acids during anaerobic mixed-culture fermentation. Water Res. 183, 115958.
Bhat, M.Y., Dar, T.A., Singh, L.R., 2016. Milk Proteins–From Structure to Biological Properties and Health Aspects. Intech Open, InTech, Rijeka, pp. 1–17.
Bourassa, P., Kanakis, C.D., Tarantilis, P., Pollissiou, M.G., Tajmir-Riahi, H.A., 2010. Resveratrol, genistein, and curcumin bind bovind serum albumin. J. Phys. Chem. B 114, 3348–3354.
Braguglia, C.M., Gallipoli, A., Gianico, A., Pagliaccia, P., 2018. Anaerobic bioconversion of food waste into energy: a critical review. Bioresour. Technol. 248, 37–56.
Breure, A.M., Van Andel, J.G., 1984. Hydrolysis and acidogenic fermentation of a protein, gelatin, in an anaerobic continuous culture. Appl. Microbiol. Biotechnol. 20 (1984), 40–45.
Breure, A.M., Beeftink, H.H., Verkuijlen, J., van Andel, J.G., 1986. Acidogenic fermentation of protein/carbohydrate mixtures by bacterial populations adapted to one of the substrates in anaerobic chemostat cultures. Appl. Microbiol. Biotechnol. 23, 245–249.
Deng, Z., Muñoz Sierra, J., Ferreira, A.L.M., Cerqueda-Garcia, D., Spanjers, H., van Lier, J.B., 2023. Effect of Operational Parameters on the Performance of an Anaerobic Sequencing Batch Reactor (AnSBR) Treating Protein-Rich Wastewater. Department of Water Management, Delft University of Technology. Under review.
Dickinson, E., 2003. Advanced Dairy Chemistry—1 Proteins. Springer, pp. 1229–1260.
Duong, T.H., Grolle, K., Nga, T.T.V., Zeeman, G., Temmink, H., van Eekert, M., 2019. Protein hydrolysis and fermentation under methanogenic and acidifying conditions. Biotechnol. Biofuels 12, 254.
Duong, T.H., van Eekert, M., Grolle, K., Tran, T.V.N., Zeeman, G., Temmink, H., 2022. Effect of carbohydrates on protein hydrolysis in anaerobic digestion. Water Sci. Technol. 86 (1), 66–79.
Elbeshbishy, E., Nakhla, G., 2012. Batch anaerobic co-digestion of proteins and carbohydrates. Bioresour. Technol. 116, 170–178.
Eurostats, 2018. Agriculture, Forestry and Fishery Statistics 2018 Edition.
FAO, 2020. World Food and Agriculture - Statistical Yearbook 2020.
Glenn, A.R., 1976. Production of extracellular proteins by bacteria. Ann. Rev. Microbiol. 30, 41–62.
GMIA, 2019. Gelatine Handbook. Gelatin Manufacturers Institute of America, US.

Guo, H., Oosterkamp, M.J., Tonin, F., Hendriks, A., Nair, R., van Lier, J.B., de Kreuk, M. K., 2021. Reconsidering hydrolysis kinetics for anaerobic digestion of waste activated sludge applying cascade reactors with ultra-short residence times. Water Res. 202 (1), 117398.
Holliger, C., Alves, M., Andrade, D., Angelidaki, I., Astals, S., Baier, U., Bougrier, C., Buffiere, P., Carballa, M., de Wilde, V., Ebertseder, F., Fernandez, B., Ficara, E., Fotidis, I., Frigon, J.C., de Laclos, H.F., Ghasimi, D.S., Hack, G., Hartel, M., Heerenklage, J., Horvath, I.S., Jenicek, P., Koch, K., Krautwald, J., Lizasoain, J., Liu, J., Mosberger, L., Nistor, M., Oechsner, H., Oliveira, J.V., Paterson, M., Pauss, A., Pommier, S., Porqueddu, I., Raposo, F., Ribeiro, T., Rusch Pfund, F., Stromberg, S., Torrijos, M., van Eekert, M., van Lier, J.B., Wedwitschka, H., Wierinck, I., 2016. Towards a standardization of biomethane potential tests. Water Sci. Technol. 74 (11), 2515–2522.
Jiang, Y., McAdam, E., Zhang, Y., Heaven, S., Banks, C., Longhurst, P., 2019. Ammonia inhibition and toxicity in anaerobic digestion: a critical review. J. Water Process. Eng. 32, 100899.
Jones, W.J., Nagle Jr., D., Whitman, W.B., 1987. Methanogens and the diversity of archaebacteria. Microbiol. Rev. 51 (1), 135–177.
Kobayashi, T., Wu, Y.P., Lu, Z.J., Xu, K.Q., 2015. Characterization of anaerobic degradability and kinetics of harvested submerged aquatic weeds used for nutrient phytoremediation. Energies 8 (1), 304–318.
Kovács, E., Wirth, R., Maróti, G., Bagi, Z., Rákhely, G., Kovács, K.L., 2013. Biogas production from protein-rich biomass: fed-batch anaerobic fermentation of casein and of pig blood and associated changes in microbial community composition. PLoS One 8 (10), e77265.
Kovács, E., Wirth, R., Maroti, G., Bagi, Z., Nagy, K., Minarovits, J., Rakhely, G., Kovács, K.L., 2015. Augmented biogas production from protein-rich substrates and associated metagenomic changes. Bioresour. Technol. 178, 254–261.
van Lier, J.B., Mahmoud, N., Zeeman, G., 2020. In: Chen, G.H., van Loosdrecht, M.C.M., Ekama, G.A., Brdjanovic, D. (Eds.), Biological Wastewater Treatment, Principles, Modelling and Design, 2nd edition. IWA Publishing, London, UK, pp. 701–756.
Liu, Y., Ngo, H.H., Guo, W., Peng, L., Wang, D., Ni, B., 2019. The roles of free ammonia (FA) in biological wastewater treatment processes: a review. Environ. Int. 123, 10–19.
Liu, L., Yun, S., Ke, T., Wang, K., An, J., Liu, J., 2023. Dual utilization of aloe peel: Aloe peel-derived carbon quantum dots enhanced anaerobic co-digestion of aloe peel. Waste Manag. 159, 163–173.
Mata-Alvarez, J., Dosta, J., Romero-Güiza, M.S., Fonoll, X., Peces, M., Astals, S., 2014. A critical review on anaerobic co-digestion achievements between 2010 and 2013. Renew. Sust. Energ. Rev. 36, 412–427.
McInerney, M.J., 1988. Anaerobic hydrolysis and fermentation of fats and proteins. In: Biology of Anaerobic Organisms, pp. 373–416.
Meegoda, J.N., Li, B., Patel, K., Wang, L.B., 2018. A Review of the Processes, Parameters, and Optimization of Anaerobic Digestion. Int. J. Environ. Res. Public Health 15 (10).
Miniaci, M.C., Irace, C., Capuozzo, A., Piccolo, M., Di Pascale, A., Russo, A., Lippiello, P., Lepre, F., Russo, G., Santamaria, R., 2016. Cysteine prevents the reduction in keratin synthesis induced by iron deficiency in human keratinocytes. J. Cell. Biochem. 117 (2), 402–412.
Nightingale, A., Antunes, R., Alpi, E., Bursteinas, B., Gonzales, L., Liu, W., Luo, J., Qi, G., Turner, E., Martin, M., 2017. The proteins API: accessing key integrated protein and genome information. Nucleic Acids Res. 45 (W1), 539–544.
Numata, K., 2021. Biopolymer Science for Proteins and Peptides. Elsevier.
Pavlostathis, S.G., Giraldo-Gomez, E., 1991. Kinetics of anaerobic treatment. Water Sci. Technol. 24 (8), 35–59.
Rajagopal, R., Massé, D.I., Singh, G., 2013. A critical review on inhibition of anaerobic digestion process by excess ammonia. Bioresour. Technol. 143, 632–641.
Ruiz, I., Veiga, M.C., de Santiago, P., Blazquez, R., 1997. Treatment of slaughterhouse wastewater in a UASB reactor and an anaerobic filter. Bioresour. Technol. 60, 251–258.
Salminen, E., Rintala, J., 2002. Anaerobic digestion of organic solid poultry slaughterhouse waste a review. Bioresour. Technol. 83, 13–26.
Siegert, I., Banks, C.J.P.B., 2005. The effect of volatile fatty acid additions on the anaerobic digestion of cellulose and glucose in batch reactors. Process Biochem. 40 (11), 3412–3418.
Slavov, A.K., 2017. Dairy wastewaters – general characteristics and treatment possibilities – a review. Food Technol. Biotechnol. 55 (1), 14–28.
Smith, G.S., Walter, G.L., Walker, R.M., 2013. Clinical pathology in non-clinical toxicology testing. In: *Haschek and Rousseaux's Handbook of Toxicologic Pathology*. Academic Press, pp. 565–594.
Tan, L.C., Peschard, R., Deng, Z., Ferreira, A.L.M., Lens, P.N.L., Pacheco-Ruiz, S., 2021. Anaerobic digestion of dairy wastewater by side-stream membrane reactors: Comparison of feeding regime and its impact on sludge filterability. Environ. Technol. Innov. 22, 101482.
Varga, N., Hornok, V., Sebok, D., Dekany, I., 2016. Comprehensive study on the structure of the BSA from extended-to aged form in wide (2−12) pH range. Int. J. Biol. Macromol. 88, 51–58.
Vivekanand, V., Mulat, D.G., Eijsink, V.G.H., Horn, S.J., 2018. Synergistic effects of anaerobic co-digestion of whey, manure and fish ensilage. Bioresour. Technol. 249, 35–41.
Wang, Y., Zhang, Y., Wang, J., Meng, L., 2009. Effects of volatile fatty acid concentrations on methane yield and methanogenic bacteria. Biomass Bioenergy 33 (5), 848–853.
Wang, L., Hao, J., Wang, C., Li, Y., Yang, Q., 2022. Carbohydrate-to-protein ratio regulates hydrolysis and acidogenesis processes during volatile fatty acids production. Bioresour. Technol. 355, 127266.
Yang, J., Molouk, A.F.S., Okanishi, T., Muroyama, H., Matsui, T., Eguchi, K., 2015. A stability study of Ni/Yttria-stabilized zirconia anode for direct ammonia solid oxide fuel cells. ACS Appl. Mater. Interfaces 7 (51), 28701–28707.
Yu, H., Fang, H.H.P., 2001. Acidification of mid-and high-strength dairy wastewaters. Water Res. 35 (15), 3697–3705.
Zhou, M., Yan, B., Wong, J.W.C., Zhang, Y., 2018. Enhanced volatile fatty acids production from anaerobic fermentation of food waste: a mini-review focusing on acidogenic metabolic pathways. Bioresour. Technol. 248, 68–78.